

# Scalable and Modular 8-Channel Transmit and 8-Channel Flexible Receive Coil Array for $^{19}\text{F}$ -MRI of Large Animals

Ali Caglar Özen<sup>1, 1</sup>, Felix Spreter<sup>1</sup>, Waldemar Schimpf<sup>1</sup>, Johannes Fischer<sup>1</sup>, Serhat Ilbey<sup>1</sup>, Simon Reiss<sup>1</sup>, Alexander Maier<sup>2</sup>, Dominik von Elverfeldt<sup>1</sup>, Timo Heidt<sup>2</sup>, Constantin von zur Mühlen<sup>2</sup>, Michael Bock<sup>1</sup>

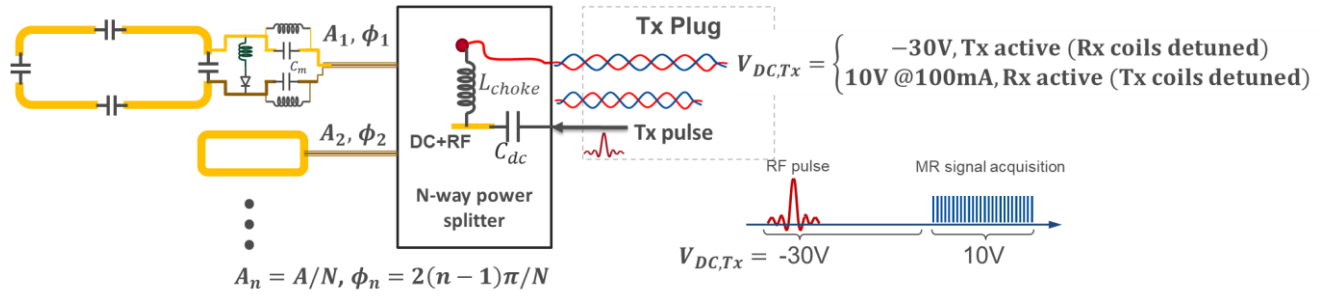
<sup>1</sup>Dept. of Radiology, Medical Physics, Medical Center – University of Freiburg, University of Freiburg, Freiburg, Germany

<sup>2</sup>Cardiology and Angiology I, University Heart Center, Medical Center University of Freiburg, Faculty of Medicine, University of Freiburg, Freiburg, Germany

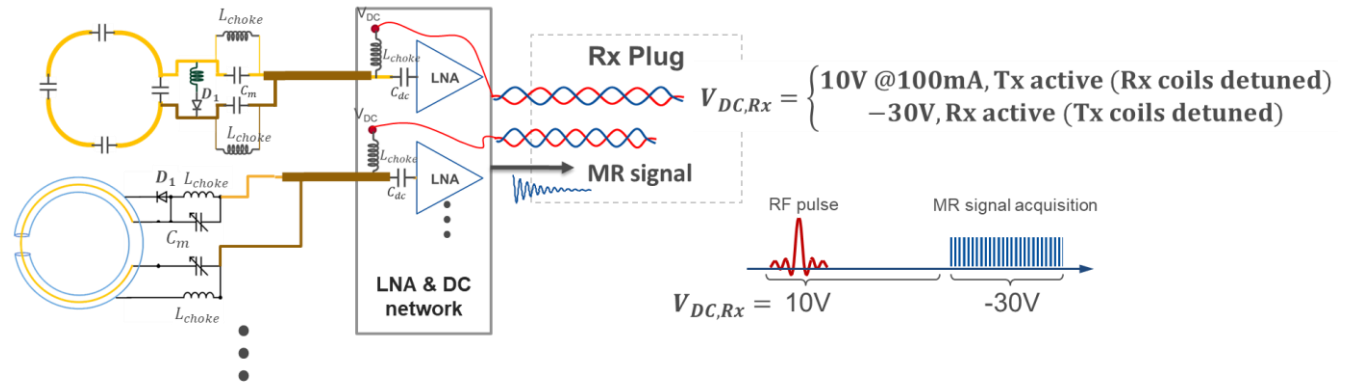
---

<sup>1</sup> Corresponding author  
Email address: [ali.oezen@uniklinik-freiburg.de](mailto:ali.oezen@uniklinik-freiburg.de)  
Tel: +49 761 270-93910  
Fax: +49 761 270-93900

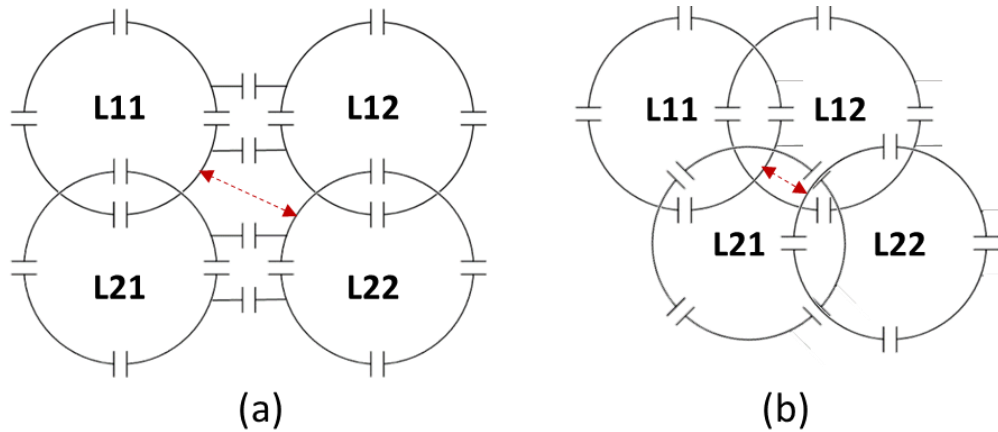
## Supplementary Material



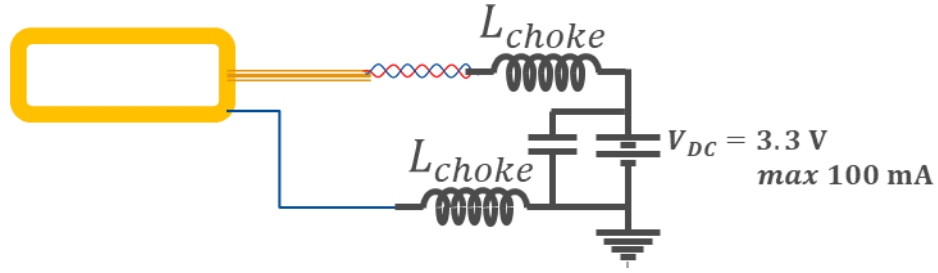
Supporting Information Fig. S1: A schematic diagram for interfacing the Tx array to the MRI system. A coil plug (Tx plug) was used to deliver the RF power from a broadband RPA, as well as the DC bias voltage for active detuning of the individual Tx coil elements, as shown in the detuning circuit for the first element. The detuning logic is predefined in the coil files, which is controlled via the RF excitation and signal acquisition entries in the pulse sequence. To avoid excessive cabling, the DC signals were coupled to the RF paths leading to the individual Tx coil elements at the power splitter.



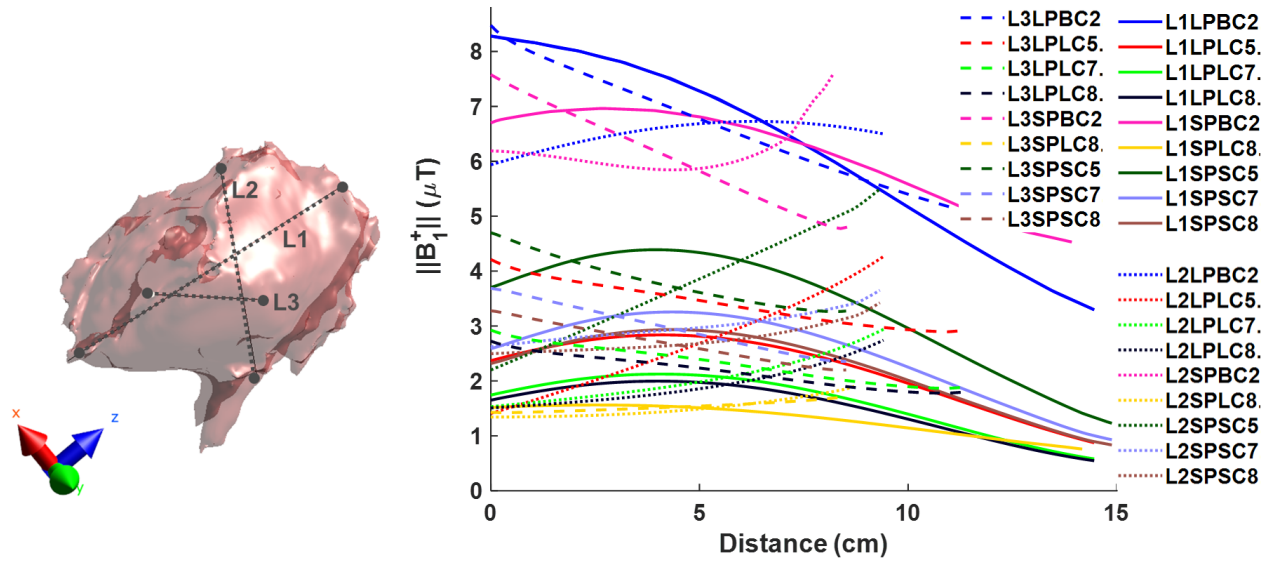
Supporting Information Fig. S2: A schematic diagram for interfacing the Rx coils to the MRI system. A coil plug (Rx plug) was used to deliver the amplified MR signal to the receiver unit of the MRI system, as well as the DC bias voltage for active detuning of the individual Rx coil elements. Detuning circuits for loop and SLR elements are shown for the first elements. An additional cross-diode is used at the preamplifier inputs (not shown) after the DC-blocking capacitor,  $C_{dc}$ , for passive protection. Preamplifiers were biased through the "MR signal" path, which is a coaxial cable with a DC signal coupled, that is activated during the receive cycle. The detuning logic is predefined in the coil files, which is controlled via the RF excitation and signal acquisition entries in the pulse sequence. To avoid excessive cabling, the DC signals for active detuning were also coupled to the RF paths on the coil side.



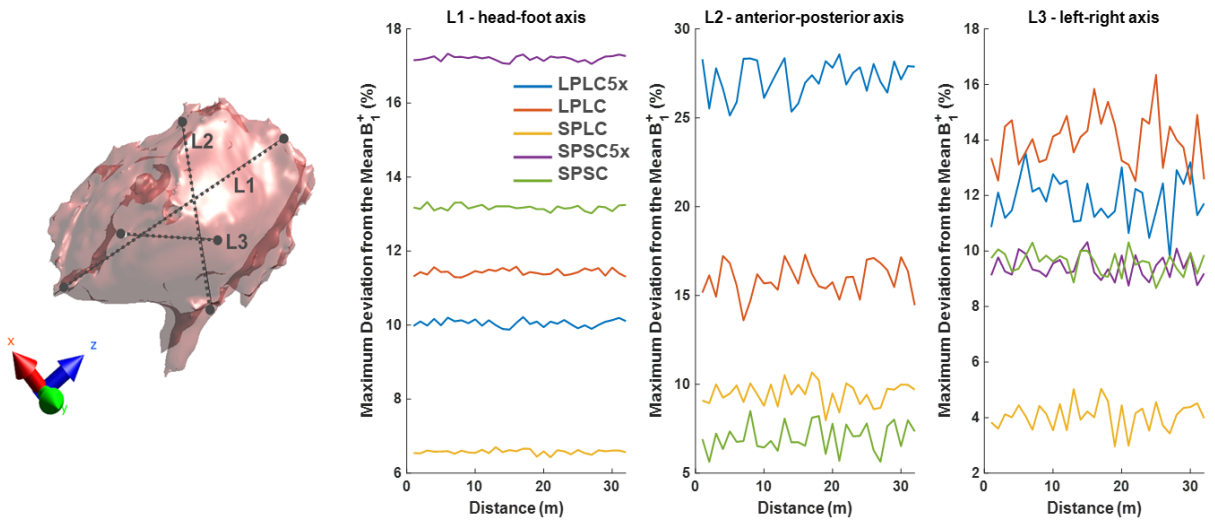
Supporting Information Fig. S3: Comparison of the next-nearest-neighbor distances in the four-loop array 2x2 configurations. The proposed approach in (a) results in a distance of 5.5cm between L11 and L22, whereas the arrangement in (b) a distance of 1.4cm. Additional decoupling of 4.3dB between L11 and L22 is gained by choosing (a) over (b).



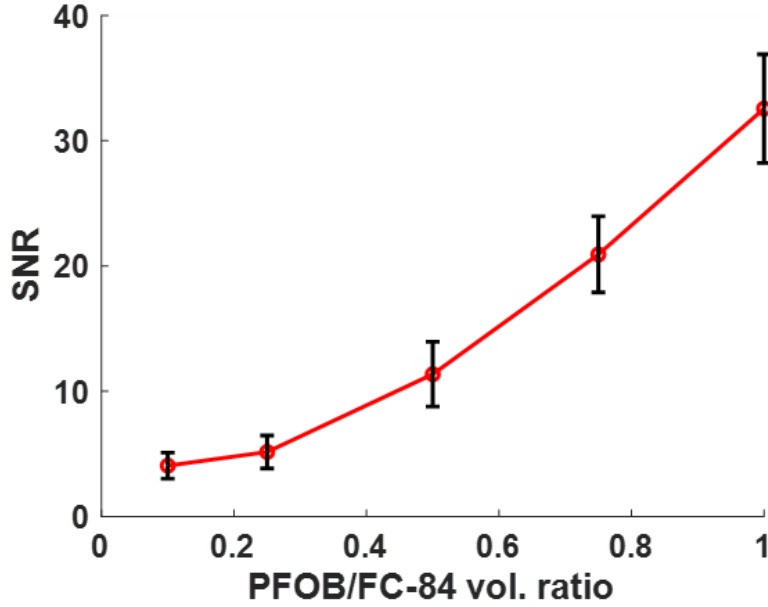
Supporting Information Fig. S4: A schematic diagram of the battery supplied detuning used for the unplugged  $^{19}\text{F}$  coils that are however left inside the magnet bore during  $^1\text{H}$  measurements. The battery output is simply connected to the coaxial cable of the  $^{19}\text{F}$  coils elements thereby activating the detuning PIN diode to minimize coupling to the  $^1\text{H}$  coils.



Supporting Information Fig. S5: Line profile results of the simulations for various pig model and coil pairs in ideal input matching case normalized to 1kW input power. Magnitude of the  $B_1^+$  field was plot along the lines in L1, head-foot, L2, anterior-posterior, and L3, right-left directions for each combination.



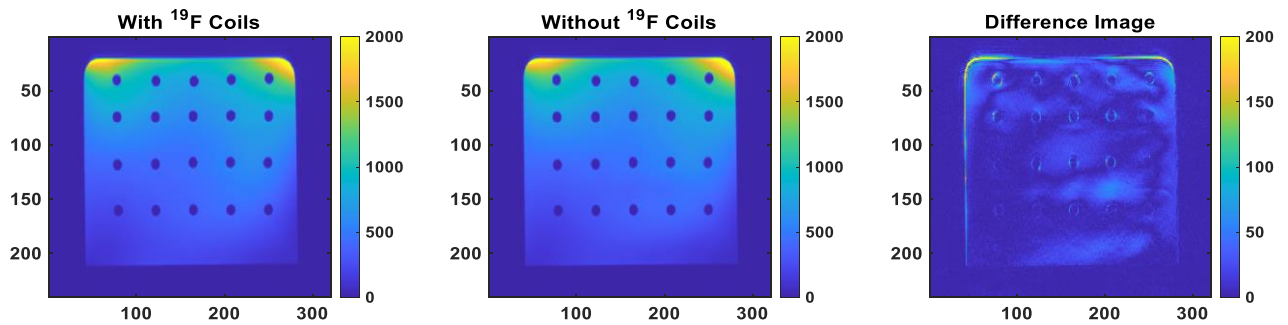
Supporting Information Fig. S6: Effect of the phase and amplitude mismatches on the  $B_1^+$  homogeneity. 32 random amplitude and phase values within 20% of the ideal values were used to calculate field distributions and maximum deviation from the mean along the lines in L1, head-foot, L2, anterior-posterior, and L3, right-left directions.



Supporting Information Fig. S7: PFOB was mixed with FC-84 (Perfluoroheptane) to test sensitivity of the coils by exciting only the CF<sub>2</sub>Br peak of PFOB using a narrow-band (3kHz) Gaussian RF pulse. The image SNR for a 2mm-isotropic FLASH sequence (32 averages) was less than 10 for the 5ml tubes with 10% and 25% solutions.

## Comparison of 1H images with and without 19F coils

To test the effect of the existing <sup>19</sup>F coils during <sup>1</sup>H MRI, image of the grid phantom was acquired with and without the <sup>19</sup>F elements and the difference image and the structural similarity index were calculated. Existing <sup>19</sup>F coils didn't have a significant effect on the <sup>1</sup>H images as shown in Supporting Information Figure S8. Structural similarity index (SSIM) and normalized mean square error (NMSE) of the transverse <sup>1</sup>H images with and without the <sup>19</sup>F coils was calculated as 0.9913 and 0.55%, respectively. There is an edge enhancement in the difference image, which can be attributed to a shift in the phantom position during removal of the posterior loop coils.



Supporting Information Fig. S8: Comparison of 1H GRE images with and without the remaining 19F elements, which were actively detuned. No significant artefacts or sensitivity change was observed with SSIM of 0.9913 and NMSE of 0.55%.